A&A 411, L377–L382 (2003)
DOI: 10.1051/0004-6361:20031324

Astronomy & Astrophysics

SPI/INTEGRAL observation of the Cygnus region

L. Bouchet[1], E. Jourdain[1], J. P. Roques[1], P. Mandrou[1], P. von Ballmoos[1], S. Boggs[8], P. Caraveo[4], M. Cassé[3], B. Cordier[3], R. Diehl[2], P. Durouchoux[3], A. von Kienlin[2], J. Knodlseder[1], P. Jean[1], P. Leleux[5], G. G. Lichti[2], J. Matteson[7], F. Sanchez[5], S. Schanne[3], V. Schoenfelder[2], G. Skinner[1], A. Strong[2], B. Teegarden[9], G. Vedrenne[1], and C. Wunderer[2]

[1] Centre d'Étude Spatiale des Rayonnements, CNRS/UPS, BP 4346, 31028 Toulouse, France
[2] Max-Planck-Institut für Extraterrestrische Physik, Postfach 1603, 85740 Garching, Germany
[3] DSM/DAPNIA/Sap, CEA-Saclay, 91191 Gif-sur-Yvette, France
[4] IASF, via Bassini 15, 20133 Milano, Italy
[5] IFIC, University of Valencia, 50 avenida Dr. Moliner, 46100 Burjassot, Spain
[6] Institut de Physique Nucléaire, Université catholique de Louvain, 1348 Louvain-La Neuve, Belgium
[7] UCSD/CASS, 9500 Gilman Drive, La Jolla, CA 92093-0111, USA
[8] Space Science Laboratory, University of California, Berkeley, CA 94720, USA
[9] Laboratory for High Energy Astrophysics, NASA/Goddard Space Flight Center, Greenbelt, MD 20771, USA

Received 17 July 2003 / Accepted 27 August 2003

Abstract. We present the analysis of the first observations of the Cygnus region by the SPI spectrometer onboard the Integral Gamma Ray Observatory, encompassing ~600 ks of data. Three sources namely Cyg X-1, Cyg X-3 and EXO 2030+375 were clearly detected. Our data illustrate the temporal variability of Cyg X-1 in the energy range from 20 keV to 300 keV. The spectral analysis shows a remarkable stability of the Cyg X-1 spectra when averaged over one day timescale. The other goal of these observations is SPI inflight calibration and performance verification. The latest objective has been achieved as demonstrated by the results presented in this paper.

Key words. gamma rays: observations – X-ray stars: individual: Cyg X-1, Cyg X-3, EXO 2030+375 – black hole: physics – space telescope: INTEGRAL: SPI

1. Introduction

The spectrometer for INTEGRAL (SPI) is one of the two main instruments onboard ESA's INTEGRAL observatory launched from Baïkonour, Kasakhstan, on October 17, 2002. The aim of SPI is to perform the high resolution spectroscopy as well as imaging of astrophysical sources in the energy range between 20 keV and 8 MeV. The imager IBIS (15 keV–10 MeV) (Ubertini et al. 1997) is complementary to SPI with its high angular resolution. JEM-X, an X-ray monitor (Westergaard et al. 1997), and OMC, an optical monitor camera (Gimenez et al. 1997), complete the INTEGRAL observatory.

The INTEGRAL observations of the Cygnus region started on 2002, November, 15 and lasted up to 2002, December, 24. Three high energy sources, namely Cyg X-1, Cyg X-3 and EXO 2030+375 were clearly detected by SPI.

Cyg X-1 is one of the brightest and most extensively studied gamma-ray sources in the sky. The system consists of a blue supergiant (HDE 226868) and a compact companion generally believed to be the prototype of a black hole candidate. Its high energy emission is characterised by a variability on time scale ranging from milliseconds to months. Cyg X-3 is a bright high-mass X-ray binary with a 4.8 hr orbital period, lying at a distance of ~10 kpc (Dickey 1983). The exact nature (black hole or neutron star) of the compact object is still in question. The companion is most likely an early Wolf-Rayet star (van Kerkwijk et al. 1992). The source is highly variable from radio to hard X-rays. It is one of the dozen Galactic binaries considered as a "microquasar" (Distefano et al. 2002).

EXO 2030+375 is a transient accreting X-ray pulsar discovered by EXOSAT during a giant outburst in 1985 (Parmar et al. 1989). Localised at ~3.6° from Cyg X-3, it is a high mass binary system consisting of a neutron star and a Be companion. Its X-ray emission is characterised by the 41.8 s neutron star pulsation coupled with recurrent outbursts occurring every 42 days and lasting 7 to 9 days, thought to mark the periastron passage of the neutron star. The most extensive observations were made by BATSE (Laycock et al. 2003) while a multi-wavelength study was performed by Wilson et al. (2002).

2. Instrument

The SPI spectrometer consists of an array of 19 actively cooled high resolution Ge detectors with an area of 508 cm^2 and a thickness of 7 cm. It is surrounded by a 5 cm thick BGO shield.

Send offprint requests to: L. Bouchet, e-mail: bouchet@cesr.fr

Table 1. INTEGRAL observations of the Cygnus region 2002 November-December.

Revolution number	Pointing mode	Date start – end Year/month/day – hh:mm	Accumulation mode	Useful duration kilosecond
11	Staring	02/11/15 – 07:17 – 02/11/18 – 07:02	photon–photon	27.8
16	Staring	02/11/30 – 06:08 – 02/12/03 – 05:54	onboard spectra	56.9
17	Staring	02/12/03 – 05:54 – 02/12/06 – 05:39	photon–photon	41.5
18	Staring	02/12/06 – 05:39 – 02/12/09 – 05:24	onboard spectra	47.4
19	Dithering	02/12/09 – 05:24 – 02/12/12 – 05:11	onboard spectra	75.7
20	Dithering	02/12/12 – 05:11 – 02/12/15 – 05:00	onboard spectra	48.5
21	Dithering	02/12/15 – 05:00 – 02/12/18 – 04:48	onboard spectra	58.0
	Dithering	02/12/15 – 05:00 – 02/12/18 – 04:48	photon–photon	39.3
22	Dithering	02/12/18 – 04:48 – 02/12/21 – 04:34	onboard spectra	123.2
23	Dithering	02/12/21 – 04:34 – 02/12/24 – 04:18	onboard spectra	75.8

The detectors cover an energy range of 20 keV–8 MeV with an energy resolution (FWHM) ranging from 2 to 8 keV as a funtion of energy. In addition to its spectroscopic capability, SPI can image the sky with a spatial resolution of about 2.6° over a field of view of 30°, thanks to its coded mask. Despite such a modest angular resolution, it is possible to locate sources within few arcminutes. See Vedrenne et al. (2003) for more details.

A complete INTEGRAL orbit lasts ∼3 days, but scientific data cannot be accumulated when the instrument is crossing the radiation belts, reducing the useful time by 30%. A detailed description of the instrument in-flight performances is given in Roques et al. (2003).

3. Observations

Each orbit consists in several exposures (typically, corresponding to the observation of a given source). Owing to the small number of detectors, imaging relies on the possibility of performing the observations in dithering mode (Vedrenne et al. 2003). The pointing direction varies in step of 2° with a 5×5 quadratic or 7 hexagonal pattern within an exposure. Each pointing has a duration generally fixed to ∼30 min.

Observations can be performed either in spectral mode, where the single events are accumulated in one unique spectrum for each pointing, or in photon-photon mode, where all events are time tagged with a temporal resolution of 102.4 μs, and stored individually.

The data used in this analysis were recorded from 2002 November 15 to 2002, December 24 (Table 1). Variations of the temperature of the Ge detectors produce a small gain drift in their associated electronics. Such an effect is easy to correct revolution per revolution, through the energy calibration of each detector using known background induced lines. For the analysis described in this paper, we used only the single detector events (see Diehl et al. 2003).

4. Data analysis

4.1. Images analysis

4.1.1. Misalignment between SPI and the star trackers

The first images of both Cyg X-1 and the Crab nebula yielded positions on average 8 arcmin away from their correct values. Such a misalignment between the star trackers and the SPI axes had been measured on ground and later found stable after launch. A correction has thus been computed and included in the data analysis. This correction is similar to that obtained by Walter et al. (2003), which was not available at the time of this analysis.

4.1.2. Background determination

The background substraction method depends on the pointing mode. For exposures in dithering mode, when a bright source illuminates a different combination of detectors in each step of the dithering pattern, it is possible to determine the background level for each detector independently. In the staring mode, the unique pointing direction makes it impossible to determine background mathematically. A model of the background distributions on the detector plane has to be assumed. Analyses of "Empty-field" observations have shown that, for a given energy, the relative count rates of the 19 Ge detectors are broadly constant while the global amplitude (normalisation factor) varies with time. We thus fix the relative count-rate distribution (depending on the energy band) leaving the normalisation as the only free parameter.

To limit the number of free parameters, we fix the background values over a timescale as long as possible. Considering the flux variations measured by the Anticoincidence Shield or Ge saturated events, we assume that the background parameters remain constant over typically half an orbit, in both staring and dithering modes.

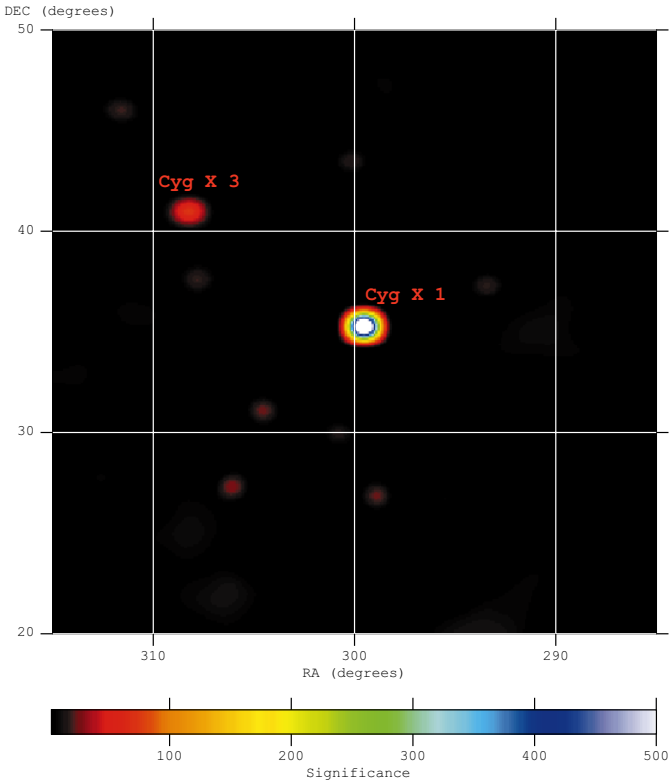

Fig. 1. An image of the Cygnus region using all data listed in Table 1 between 20 and 84 keV. The significance levels for Cyg X-1 and Cyg X-3 are 684σ and 74σ respectively.

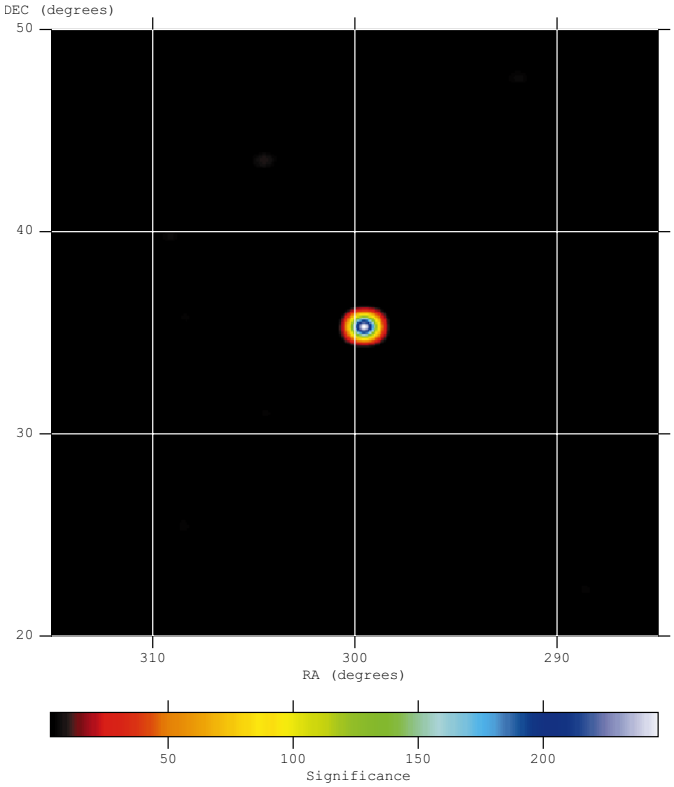

Fig. 2. An image of the Cygnus region as above between 84 and 308 keV. The significance level for Cyg X-1 is 247σ while Cyg X-3 is not detected.

4.1.3. Images

We have used an iterative source removal algorithm to build sky images (SPIROS, Skinner & Connell 2003). It is always difficult to build images with a strong and variable source. The main uncertainties come from the background determination. Although the background is generally quite stable (solar flares or radiation belts regions excepted), variations of several percents of the background along with source variability can yield unreliable results. In order to limit these effects, we have not used pointings for which reconstructed images (convolved by the reponse matrix), when compared to detector counts, give an unacceptable χ^2. Those precautions reduced the number of pointings used by ~10%. For each image, we are looking for a maximum of 10 sources or all sources above a threshold level of 2σ.

Figure 1 shows an image of the Cygnus region, in the energy range between 20 and 84 keV, obtained by SPI using all the cleaned data, i.e. ~600 ks.

It demonstrates, first of all, that our misalignment correction is valid: the SPI position for Cyg X-1 turned out to be $\alpha_{2000} = 299.559 \pm 0.016$ $\delta_{2000} = 35.202 \pm 0.012$, compatible, within less than 2 arcmin, with its known position. The statistical significance of the detection of Cyg X-1 is ~680σ (20–84 keV).

Figure 1 shows also the presence of Cyg X-3 at $\alpha_{2000} = 308.222 \pm 0.090$ $\delta_{2000} = 40.929 \pm 0.062$, compatible with the source theoretical position, with a significance of 74σ.

When selecting higher energy ranges, as in Figs. 2 and 3, reconstructed using photons in the 84–308 keV and 308–615 keV energy ranges, only Cyg X-1 continues to be detected.

Figure 4 contains only the period of activity of EXO 2030+375, namely revolution 19 to 22, with a total of 345 ks of observing time (see Sect. 4.2).

EXO 2030+375 is found at $\alpha_{2000} = 308.02 \pm 0.10\delta_{2000} = 37.55 \pm 0.08$, compatible with its known position.

In Fig. 4 (20–50 keV), the statistical significance of sources is as follows: Cyg X-1 is detected at 570σ, Cyg X-3 at 86σ and EXO 2030+375 at 36σ.

All the other excesses are found with a significance less than 15σ, i.e. less than 3% of the strongest source. The presence of noise at this level can be explained in terms of Cyg X-1 variability, background determination procedure, and/or systematic effects due to uncertainties in the calculated coded mask response.

4.2. Light curves

The light curves of the three sources are obtained simultaneously, with the background fixed to the mean orbit values (see Sect. 4.1.2). The source positions are left free but they are required to be constant for the whole set of observations.

For Cyg X-3 and EXO 2030+375, the pointings have been regrouped to get a timescale of ~5–6 hours.

The light curve of Cyg X-1 (Fig. 5) shows a marked variability at low energy (20–48 keV), by a factor of ~2.

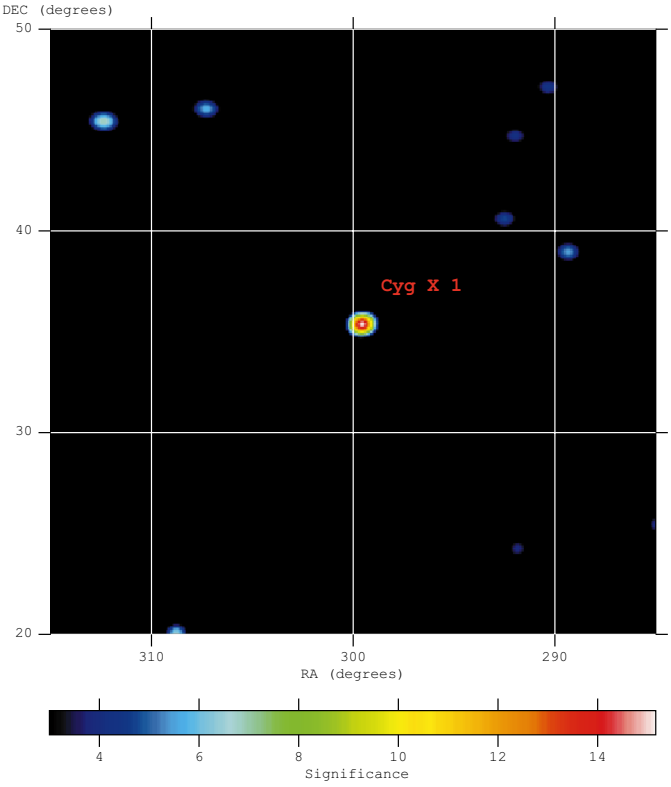

Fig. 3. An image of the Cygnus region using all data listed in Table 1 between 308 and 615 keV. The significance level for Cyg X-1 is 16σ.

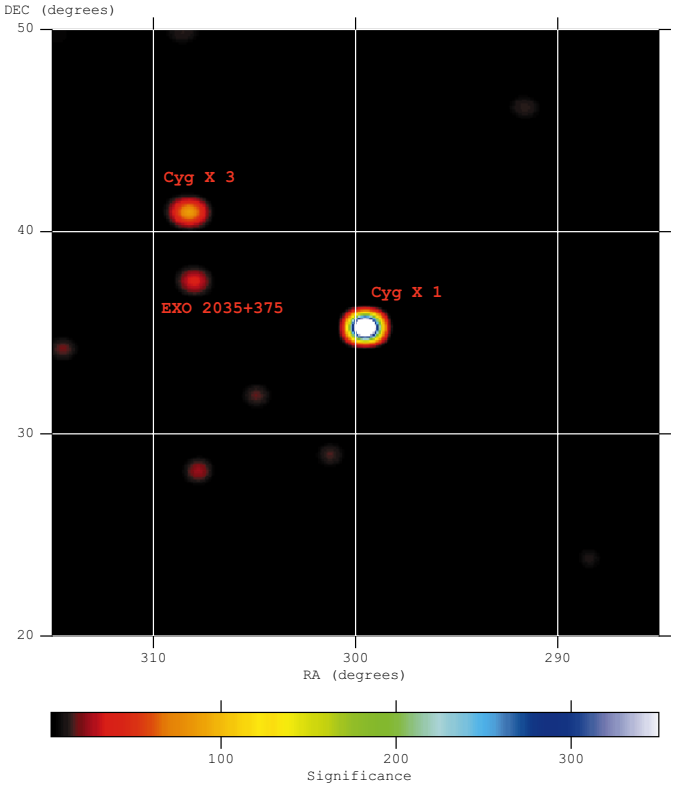

Fig. 4. Image of Cygnus region for revolutions 19 to 22 (see Table 1) in the energy range between 20 and 50 keV.

Figures 6 and 7 show the light curves of Cyg X-3 and EXO 2030+375 between 20 and 45 keV. Although the statistics are much less impressive than in the case of Cyg X-1, we can see that Cyg X-3 is detected through all the revolutions, while EXO 2030+375 exhibits temporal evolution corresponding to an expected periastron outburst, with no detection before day 2002/12/09, then a significant emission from 2002/12/10 to 02/12/20 (middle of revolution 19 through revolution 22, see Table 1).

4.3. Spectra

Counts and photon spectra for all the sources in the field of view are extracted simultaneously by an algorithm which fits all the positions and intensities of a set of given sources. To build photons spectra, we need the energy response matrix corresponding to each pointing. We used 2003, May version of the energy response matrix (Sturner et al. 2003).

4.3.1. Cyg X-1

Figure 8 shows the spectrum of Cyg X-1 averaged over the total exposure time of ~600 ks.

The source is detected up to ~1 MeV and its spectrum is well described, at least up to ~300 keV, by the usual Sunyaev-Titarchuck (S-T) inverse Compton emission model (Sunyaev & Titarchuck 1980) or by a power law with an exponential cutoff. For a spherical geometry, the temperature (kT_e) is ~48 keV and the optical depth is $\tau \sim 2.5$ for the S-T model

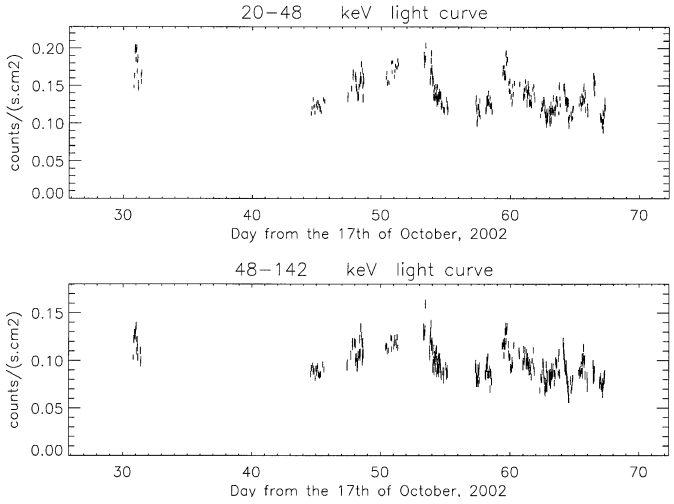

Fig. 5. The light curve of Cygnus X-1 between 20 and 48 keV and 48 and 142 keV with a time resolution of ~30 min.

while for the second model the power law index is ~1.5 and the cutoff energy ~155 keV. A thermal law gives a temperature of ~70 keV. In oder to compare our results with those obtained by OSSE/GRO, where the fitting was performed between 60 keV and 4 MeV (Phlips et al. 1996), we computed also the best fitting parameters above 60 keV. The new fit yielded higher $kT_e \sim 58$ keV with a lower optical depth $\tau \sim 2.0$, a set of parameters fully compatible with those of OSSE/CGRO.

Above 300 keV, we detect an excess with respect to the S-T model, similar to that measured by OSSE/GRO (Phlips et al. 1996). We cannot exclude that the variability of the source

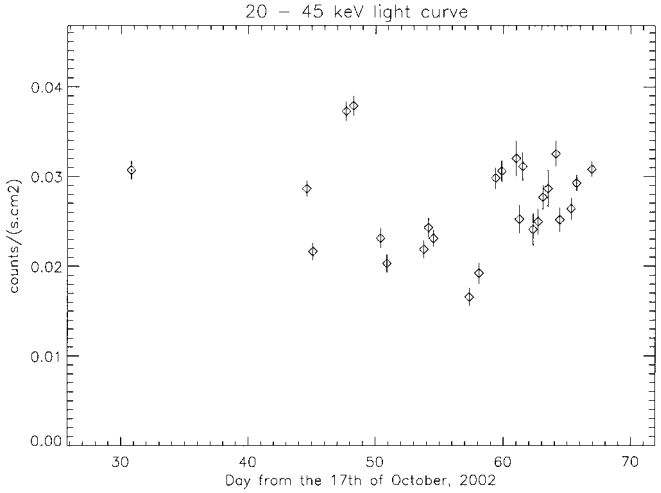

Fig. 6. Light curves of Cygnus X-3 with a time resolution of 5–6 hours (20–45 keV).

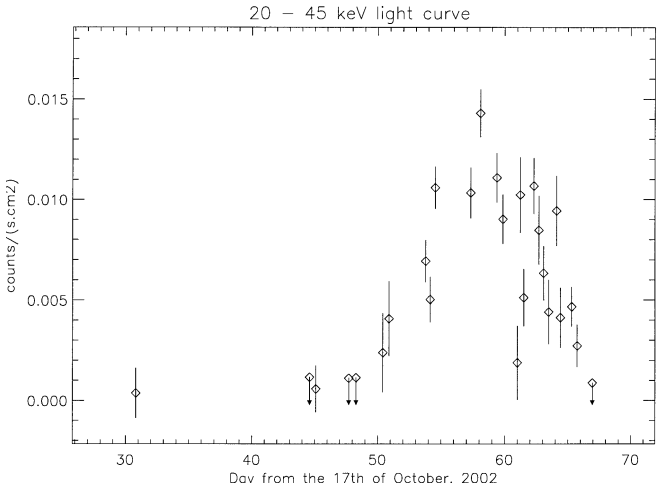

Fig. 7. Light curves of EXO 2030+375 with a time resolution of 5–6 hours (20–45 keV).

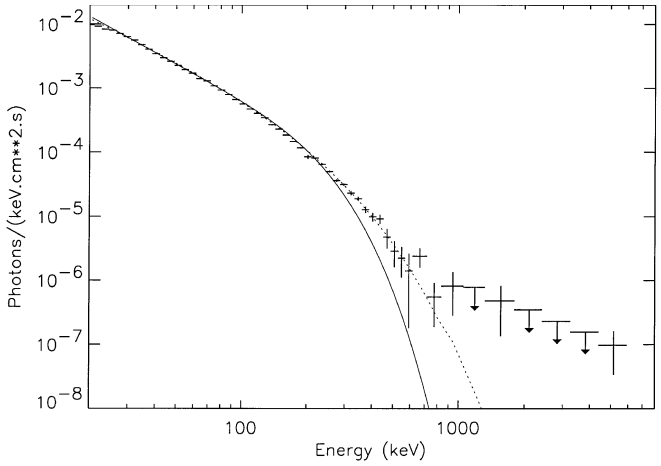

Fig. 8. Mean photon spectra of Cyg X-1 for the entire set of observations (~600 ks). Solid line is Sunyaev-Titarchuck (S-T) model and dotted line is the power law + exponential cutoff model. Upper limits are at 1σ.

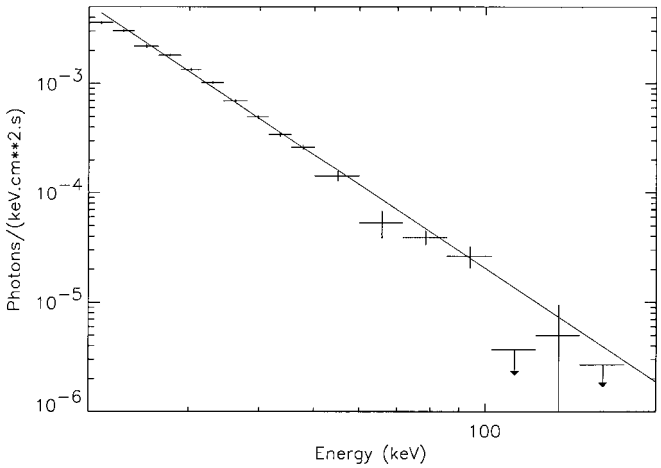

Fig. 9. The average spectrum of Cyg X-3 for a total exposition of 600 ks. The solid line is a best fit power law model, with an index of 3.45 ± 0.01 and a flux at 50 keV of 2.19 ± 0.01 × 10^{-4} photons cm^{-2} s^{-1} keV^{-1}. Upper limits are at 1σ.

produces such a feature when the data are integrated over a long time.

The individual spectra, built on timescale of one orbit, reflect the variability of the source intensity, but the spectral parameters remain remarkably stable, with kT_e varying from 5 to 54 keV and τ from 2.2 to 2.6, the power law with an exponential cutoff model gives α between 1.5 and 1.7 and a cutoff energy in the energy range 144–205 keV. We have to note that the χ^2, obviously rather high, are lower with the exponential cutoff power law model.

4.3.2. Cyg X-3

The Cyg X-3 average spectrum is shown in Fig. 9.

Cyg X-3 is detected up to ~100 keV and its average photon spectrum is well fitted by a power law of index ~3.45 with a flux at 50 keV of ~2.2×10^{-4} photons cm^{-2} s^{-1} keV^{-1}. This index value is similar to that reported by OSSE (McCollough et al. 1999), but softer than the non-thermal power law component index derived by Choudhury et al. (2002) with ASM+BATSE data.

4.3.3. EXO2030+375

EXO 2030+375 is also detected up to 150 keV (Fig. 10). Its average photon spectrum (revolution 19 to 22, 345 ks exposure) is well fitted by a thermal model with temperature ~27 keV or a power law of index ~2.7.

A possible spectral feature at ~36 keV, tentatively explained as a cyclotron absorption line, has been suggested by Reig & Coe (1999).

We do not detect this feature in the averaged spectrum with a 2σ upper limit between 34 and 38 keV of 8 × 10^{-5} ph cm^{-2} s^{-1}. We cannot exclude the presence of such a feature in shorter timescales, but this requires further analysis.

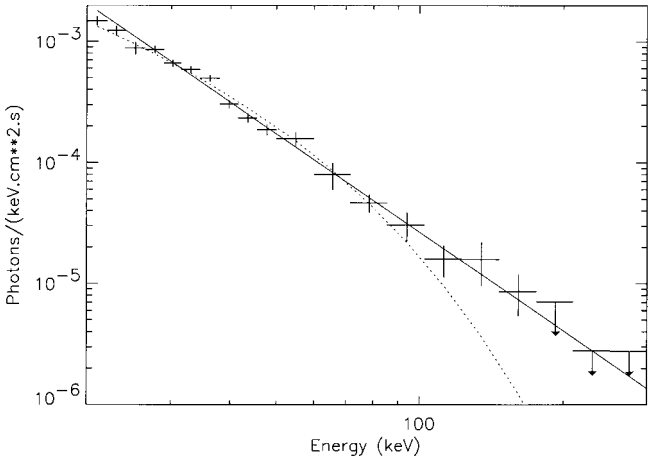

Fig. 10. The average spectrum of EXO 2030+375 for a total exposition time of 345 ks. The best fit power law (solid line) has an index of 2.72 ± 0.02 and the best fit thermal model (dotted line) has a temperature of 27.2 ± 0.1. Upper limits are at 1σ.

5. Discussion and conclusion

The emission from Cyg X-1 has been detected up to 1 MeV. While, in the energy range between 20 and 300 keV, its flux varies by a factor of ~2, its spectral shape remains remarkably stable, on a one day timescale. Our mean photon spectrum is compatible with the average CGRO/OSSE spectrum in the hard state (McConnell et al. 2002).

An outburst of EXO 2030+375 occured during our observations. The average SPI spectrum during this 6–7 days outburst is compatible with that obtained by BATSE (Wilson et al. 2002).

Initial results obtained on Cyg X-1, Cyg X-3 and EXO 2030+375 are coherent with the knowledge we have on those sources and allow us to proceed with a more detailled analysis.

Note that, although the angular distance between Cyg X-3 and EXO 2030+375 is close to the angular resolution of SPI, we can easily measure their fluxes and positions.

Cyg X-1 is one of the strongest persistent source in the SPI/INTEGRAL energy domain. From a technical point of view, it is used to test the coherence of our data analysis system, performance verification and inflight calibrations. Those objectives have been achieved and they demonstrate that SPI is working perfectly. First of all, at the present time, the quality of the images leads us to conclude that the spatial and energy responses are accurate to about 2–3%.

While qualitative results will not change, quantitative results are subject to the incertainties in the used energy response. We used the May 2003 version of the response matrix (Sturner et al. 2003), which underestimates the efficiency at low energy, resulting in steeper spectra.

We plan to improve the data analysis system by using more precise background analysis and modelling and by including source variability in the image analysis package.

Acknowledgements. The SPI/INTEGRAL project has been completed under the responsibility and leadership of CNES. We are grateful to ASI, CEA, CNES, DLR, ESA, INTA, NASA and OSTC for support.

References

Choudhury, M., Rao, A. R., Vadawale, S. V., Ishwara-Chandra, C. H., & Jain, A. K. 2002, A&A, 383, L35
Dickey, J. M. 1983, ApJ, 273, L71
Diehl, R., Baby, N., Beckmann, P., et al. 2003, A&A, 411, L117
Distefano, C., Guetta, D., Waxman, E., & Levinson, A. 2002, ApJ, 575, 378
Gimenez, A., Mas-Hesse, J. M., Jarmar, C., et al. 1997, in Proc. 2nd INTEGRAL workshop, The transparent universe, St-Malo, France ESA SP-382, 613
Laycock, S., Coe, M. J., Wilson, C. A., Harmon, B. A., & Finger, M. 2003, MNRAS, 3 38, 211
McConnell, M. L., Zdiarski, A. A., Bennett, K., et al. 2002, ApJ, 572, 984
McCollough, M. L., Robinson, C. R., Zhang, S. N., et al. 1999, ApJ, 517,951
Parmar, A. N., White, N. E., Stella, L., & Ferri, P. 1989, ApJ, 338, 359
Phlips, B. F., Jung, G. V., Leising, M. D., et al. 1996, ApJ, 465, 907
Reig, P., & Coe, M. J. 1999, MNRAS, 302, 700
Roques, J. P., Schanne, S., von Kienlin, A., et al. 2003, 411, L91
Skinner, G., & Connell, P. 2003, A&A, 411, L123
Struner, S. J., Shrader, C. R., Weidenspointner, G., et al. 2003, A&A, 411, L81
Sunyaev, R. A., & Titarchuck, L. G. 1980, A&A, 86, 121
Ubertini, P., Di Cocco, G., & Lebrun, F. 1997, in Proc. 2nd INTEGRAL workshop, The transparent universe, St-Malo, France ESA SP-382, 599
van Kerkwijk, M. H., Charles, P. A., Geballe, T. R., et al. 1992, Nature, 355, 703
Vedrenne, G., Roques, J. P., Schoenfelder, V., et al. 2003, A&A, 411, L63
Walter, R., Favre, P., Dubath, P., et al. 2003, A&A, 411, L25
Westergaard, N. J., Budtz-Jorgensen, C., Schnopper, H. W., et al. 1997, in Proc. 2nd INTEGRAL workshop, The transparent universe, St-Malo, France ESA SP-382, 615
Wilson, C. A., Finger, M. H., Coe, M. J., & Laycock, S. 2002, ApJ, 570, 287